Improving energy and time resolution of inorganic scintillators by using photonic crystals

Stuti Surani[1], Roman Samulyak[1], Federico Scurti[1], Douglas E. Wolfe[1,2], and Marek Flaska[1]

[1]Ken and Mary Alice Lindquist Department of Nuclear Engineering

[2]Department of Materials Science and Engineering

The Pennsylvania State University

Abstract

Inorganic scintillators are widely used in various gamma spectroscopy applications such as nuclear nonproliferation and safeguards, medical applications, space applications, and astronomy. They typically have good energy resolution, stable performance, low cost compared to semiconductors, and high detection efficiency. However, many inorganic scintillators have high refractive indices and suffer significant light losses due to total internal reflection (TIR). These TIR losses can be reduced by modifying the boundary conditions at the scintillator-photosensor interface. We have been assessing the use of periodic arrays of dielectric nanostructures termed photonic crystals (PHCs) to improve the overall light extraction via constructive interference. Our earlier simulation work has demonstrated that the use of 2D PHCs for LYSO and BGO 10 x 10 x 3 mm^3 scintillators should improve the light extraction by more than 60% and 90%, respectively. These simulations were done with OptiFDTD code only for a single light pass through the scintillator. Future work will include multiple light passes, allowing for even more realistic simulations. In this work, we manufacture an unoptimized PHC geometry and characterize it with radiation measurements. The manufacturing process needs to be optimized for the small PHC dimensions we require for optimized PHC production. Future work will focus on building a reliable and consistent manufacturing process that allows us to validate our model and assess the full potential of optimized PHC structures in improving the detector's performance and energy resolution. A validated simulation model will also allow us to estimate the PHC capabilities of other inorganic scintillators, such as sodium iodide and lanthanum bromide.

Keywords: photonic crystals, light extraction, inorganic scintillators, optimization

Introduction

Inorganic scintillators are widely used for gamma spectroscopy due to their good energy resolution, high light yield, stable performance, and low cost compared to semiconductors. In recent years, scintillator developments have focused on improving the energy resolution for homeland security applications and the time resolution for medical applications [1]. Inorganic scintillators are more versatile than semiconductors but typically lack the high energy resolution of semiconductors. By improving the overall light output of an inorganic scintillator, the energy and time resolutions can be improved as well [2], [3]. While most inorganic scintillators have a relatively high light yield, their ideal light output is lowered by various light loss mechanisms, including the total internal reflection (TIR) at the scintillator-photosensor interface.

Photonic crystals (PHCs) are repetitive nanostructures theorized to improve the light output of inorganic scintillators by reducing the light losses due to TIR. The nanostructures of high refractive index material act as periodic alternating dielectric media at the crystal surface as shown in Figure 1. Therefore, PHCs improve the overall collection of light photons with specific wavelengths through constructive interference and diffraction [2], [4].

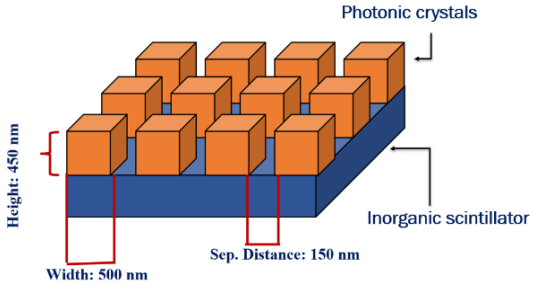

Figure 1. Schematic representation of a photonic crystal layer on a scintillator.

This project focuses on improving the light output and energy resolution from inorganic scintillators using optimized PHCs. Earlier simulation work has demonstrated an improvement in light transmission for a 10 x 10 x 3 mm^3 LYSO scintillator [5]. LYSO was chosen for the preliminary tests due to its high light yield, relatively low cost, and non-hygroscopic nature. In this paper, we will discuss the manufacturing of the optimized and unoptimized PHC geometries and the radiation measurements performed for the LYSO scintillator with and without PHCs. The preliminary experimental data indicate the effectiveness of PHCs for an unoptimized geometry. Lessons learned during this process will also be used to make the manufacturing process more reliable and consistent in future work.

Methodology

Based on their geometry, PHCs can be used to enhance the light output or increase the surface reflectiveness. For our application, we strive to optimize the PHC geometry to maximize the light output from inorganic scintillators. The preliminary tests focus on a 10 x 10 x 3 mm^3 LYSO scintillator coupled with 2D block structure Si_3N_4 PHCs. The material properties for the LYSO scintillator are given in Table 1 [6] .

Table 1. Material properties for LYSO scintillator.

Properties	LYSO
Dimensions (mm^3)	10 x 10 x 3
Refractive Index	1.81
Light Yield (photons/keV)	33
Decay Time (ns)	54

The project flowchart, shown in Figure 2 outlines our systematic approach. First, we use a Monte Carlo code, Geant4 [7] to simulate the macroscale geometry of the scintillator and the scintillation process in response to a gamma source. The second step involves modeling the light transport through the PHC structures at the nanoscale level with a deterministic code OptiFDTD [8]. OptiFDTD treats

light as electromagnetic waves, which is important for simulating the interactions with PHCs. The third step in the project is to manufacture the selected PHC geometry onto a bare 10 x 10 x 3 mm^3 LYSO using the electron beam lithography. Finally, in the last step we characterize the scintillators with and without the PHC coupling using gamma radiation measurements.

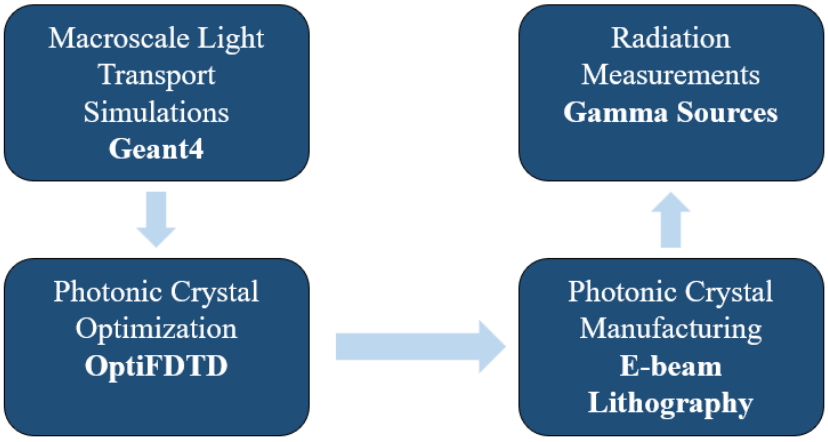

Figure 2. Project flowchart.

Simulation Methodology

For the macroscale simulations, we use Geant4, which simulates light as virtual particles called "optical photons" [9]. The code simulates a 662-keV point gamma source representative of a Cs-137 source used for the radiation measurements, as shown in Figure 3. The gamma source produces scintillation photons isotopically within the scintillator that are consistent with the emission spectrum of LYSO. The scintillation photons undergo absorption, reflection, refraction, or scattering within the scintillator before being tallied at the scintillator-photosensor interface. Material data for the simulations were obtained by UV-vis and ellipsometry measurements. The energy and angular distributions of photons at the scintillator-photosensor interface shown in Figure 4 are used as an input light source for the nanoscale simulation in OptiFDTD.

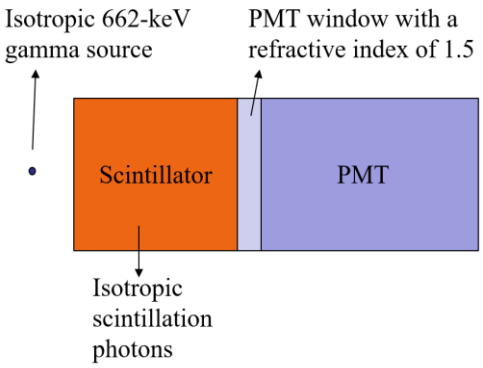

Figure 3. Schematic of the Geant4 simulation.

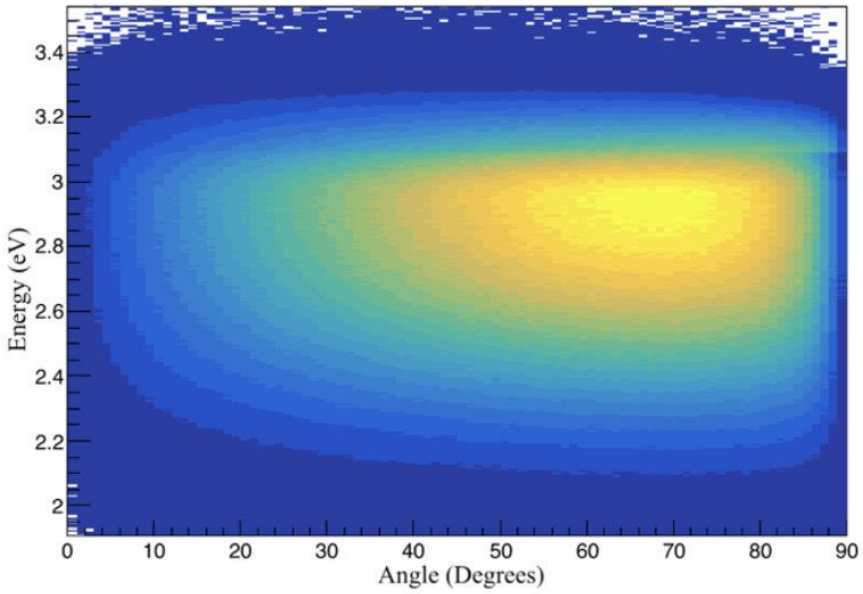

Figure 4. Energy-angular distribution for a 3-mm LYSO scintillator.

The nanoscale interaction of light cannot be accurately modeled without a complex treatment of electromagnetic waves. Therefore, the deterministic code OptiFDTD is used to model light as electromagnetic waves. It is based on the finite-difference time-domain (FDTD) simulation approach [10]. The algorithm solves both the electric and magnetic fields in temporal and spatial domains using the full-vector differential form of Maxwell's coupled curl equations. We simulated 2D block structure PHC geometries during our preliminary investigations, as shown in Figure 5. The scintillator material is LYSO and the PMT material is modeled with a refractive index of 1.5. The model currently only simulates the first passage of light through the scintillator-photosensor interface. Any subsequent light that comes back after multiple reflections is not accounted for. The light transmission is optimized by varying the thickness of the PHC (PHC z), the length of the PHC (PHC x) and the spacing between the PHCs (Gap). These three parameters are varied from 0.1 um to 1 um for 10 iterations each. The input source calculated from Geant4 is located within the scintillator, and the transmission is calculated within the PMT.

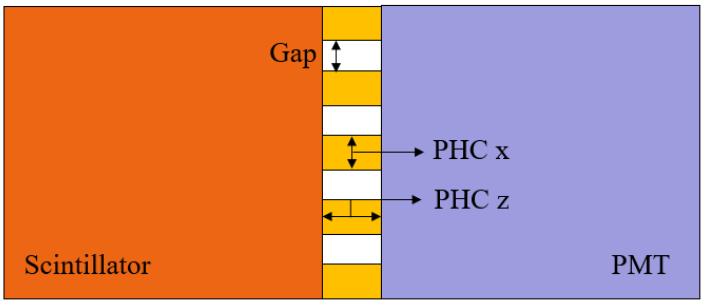

Figure 5. Schematic of PHC geometry in OptiFDTD.

PHC Manufacturing Methodology

The manufacturing process selected is the electron beam lithography due to its high spatial resolution. It is also an industry-available technology that can be scaled up for manufacturing if required. The initial tests focus on the electron beam lithography and dry etching to replicate the modeled geometry. PHCs can be made from any dielectric material with a higher refractive index than the refractive index of the scintillator itself. Examples of such materials are TiO_2, HfO_2, and Si_3N_4. For LYSO, we chose Si_3N_4 for its refractive index of approximately 2.01 at 415 nm, relative to the refractive index of LYSO (1.83). The complete PHC manufacturing methodology is shown in Figure 6.

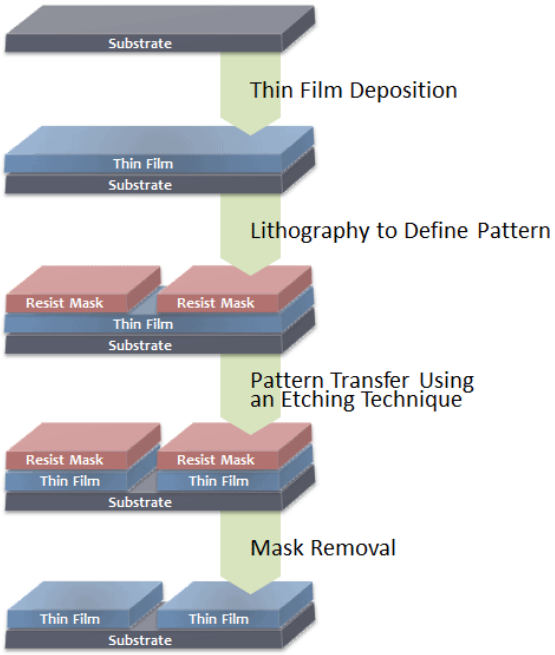

Figure 6. Flowchart for manufacturing the PHCs using electron beam lithography and ion etching.

We first perform radiation baseline measurements to provide a reference light yield and energy resolution for a bare 10 x 10 x 3 mm^3 LYSO scintillator. After cleaning the crystals, a 300-nm Si_3N_4 film is deposited onto the scintillator using radio frequency (RF) reactive sputtering at room temperature. Next, we deposit a resist layer, or polymer-based film, using spin casting onto the surface of the silicon nitride. A thin gold layer is also deposited via thermal evaporation to aid in conductivity during the electron beam writing process to help mitigate charge build-up. Next, a Raith EBPG5200 electron beam lithography tool is used to create the PHC pattern into the photoresist to cure. After electron beam lithography, the photoresist is developed, the gold layer is removed, and a Ni layer is deposited as a hard mask. The sample is then transferred into a reactive ion etch chamber to mill or etch away the silicon nitride, leaving behind the pillar geometry. At this stage, we do SEM measurements to measure the feature PHC dimensions. Finally, the nickel layer is lifted to reveal the PHC pattern on the substrate.

Radiation Measurements Setup

After the PHC manufacturing, the LYSO scintillators coupled with PHCs are characterized with radiation measurements. The radiation measurements utilize four 5-uCi ^{137}Cs gamma sources coupled together. The experimental geometry is shown in Figure 7. The scintillator is placed on a Hamamatsu H10580 PMT and kept stable using a 3D-printed PMT holder. The PMT is connected to a CAEN DT5730 digitizer [11], which processes the analog signals from the PMT and converts them to digital signals processed by a computer software CoMPASS [12] by CAEN. The PMT voltage is kept constant at -1200 volts.

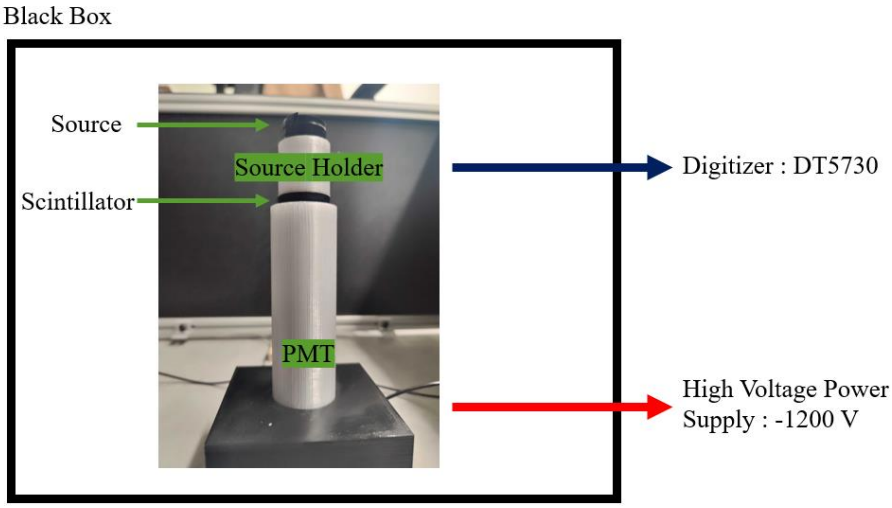

Figure 7. Radiation measurements setup.

At this point, the scintillator responses are measured without any optical coupling and surface reflectors to avoid any surface contamination that could worsen the quality of the PHC manufacturing process itself. The objective of these tests is to compare the bare scintillator versus and the PHC deposited scintillator under the same conditions, to assess the impact of the PHCs. Measurements are performed such that the Cs-137 photopeak has at least 100,000 counts.

Results and Discussion

The PHC optimization simulations for a single light pass in a 10 x 10 x 3 mm^3 LYSO scintillator are shown in Figure 8. Three optimized PHC geometries are selected for manufacturing as shown in Table 2. Only the gap parameter is changed since it determines the manufacturing resolution needed. The lower the gap value, the higher the manufacturing resolution required. With these three geometries, we produced five PHC LYSO samples L22-L26 as shown in Table 2: L22 and L23 for a gap of 0.5 um, L24 for a gap of 0.22 um, and L25 and L26 for a gap of 0.7 um. The LYSO samples were characterized with baseline radiation measurements before manufacturing.

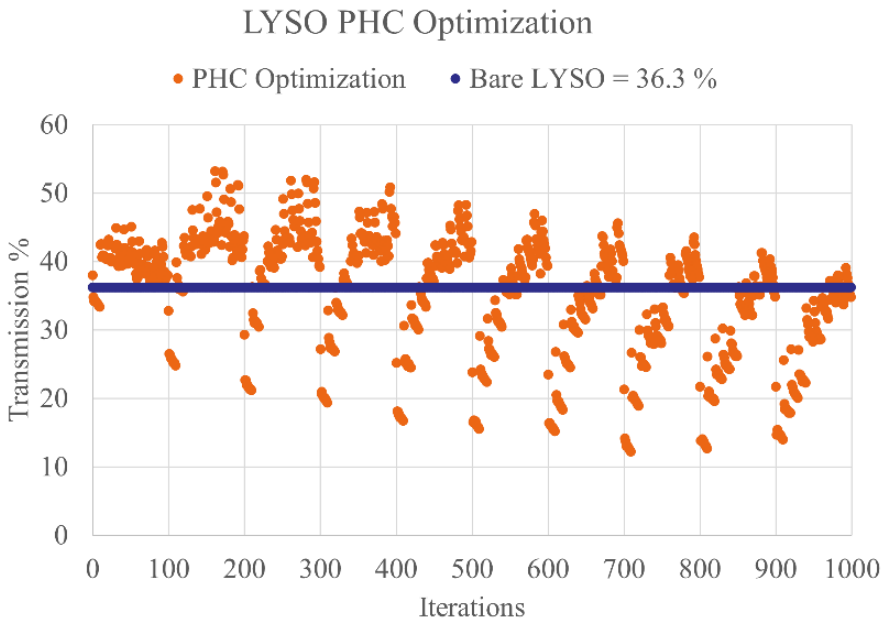

Figure 8. PHC optimization simulation results for LYSO scintillator.

Table 2. Optimized PHC geometries for manufacturing.

	Sample #	Gap (um)	PHC x (um)	PHC z (um)	Transmission	Improvement
1	L24	0.22	1	0.3	59%	63%
2	L22,L23	0.5	1	0.3	48%	33%
3	L25,L26	0.7	1	0.3	46%	26%

SEM measurements are performed for the manufactured samples post-ion etching, as shown in Figure 9. The ion etching was unsuccessful for the higher-resolution samples with lower gap values. The electron beam lithography process needs to be optimized for these structures in future work. For samples L25 and L26, the ion etching was successful, and these samples were then used in radiation measurements.

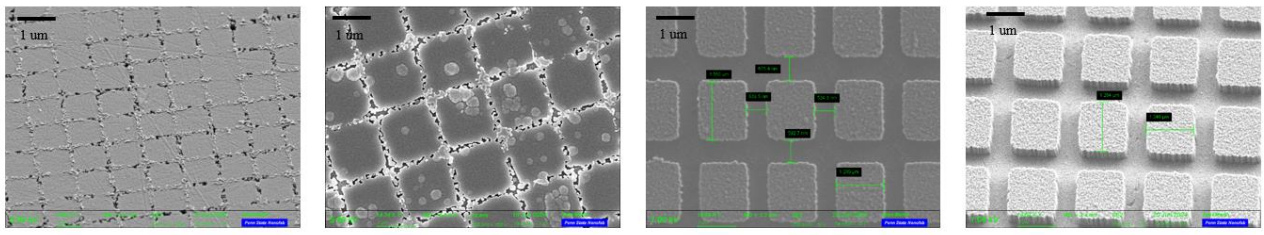

Figure 9. SEM measurements for manufactured PHC LYSO crystals.

For the samples L25 and L26, SEM imaging shows that while ion etching was successful, the PHC dimensions deviated from the target geometry as shown in Figure 10 for L26. The target PHC thickness was set to 0.3 um. However, while the target PHC gap was set to 0.7 um, the manufactured gap is approximately 0.55 – 0.65 um. Regarding the target PHC length set to 1 um, the actual measured length is approximately 1.2-1.4 um.

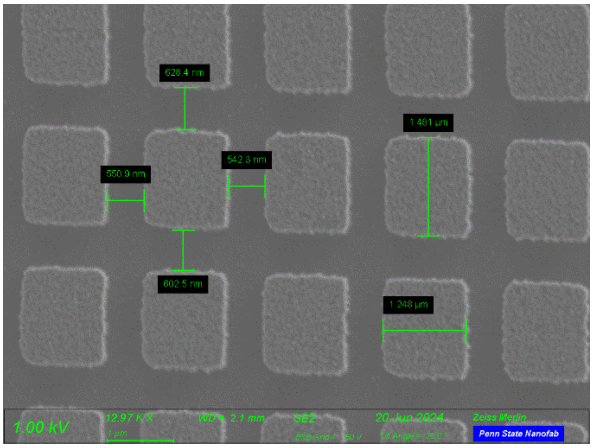

Figure 10. SEM measurement for sample L26.

Another observed manufacturing issue was caused by using Kapton tape during the PHC depositions, which led to reduced PHC coverage at 60-70% because of edge defects as shown in Figure 11. These issues are being resolved in the next round of PHC manufacturing, and it is our objective to achieve a PHC coverage of at least 90% for improved light collection.

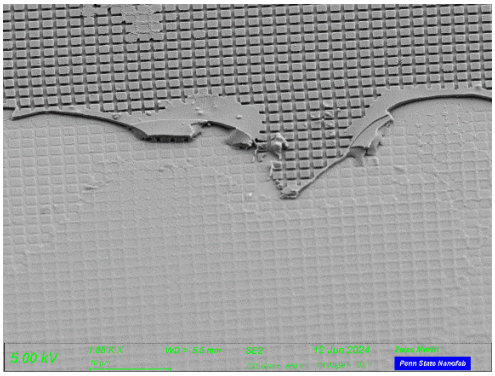

Figure 11. Edge defects in manufactured PHC LYSO crystals.

Hence, although the samples L25 and L26 were successful in terms of ion etching, they deviate from the originally proposed PHC geometry and have substantially less PHC coverage. We performed Cs-137 radiation measurements for the samples L25 and L26 and the results are shown in Figure 12.

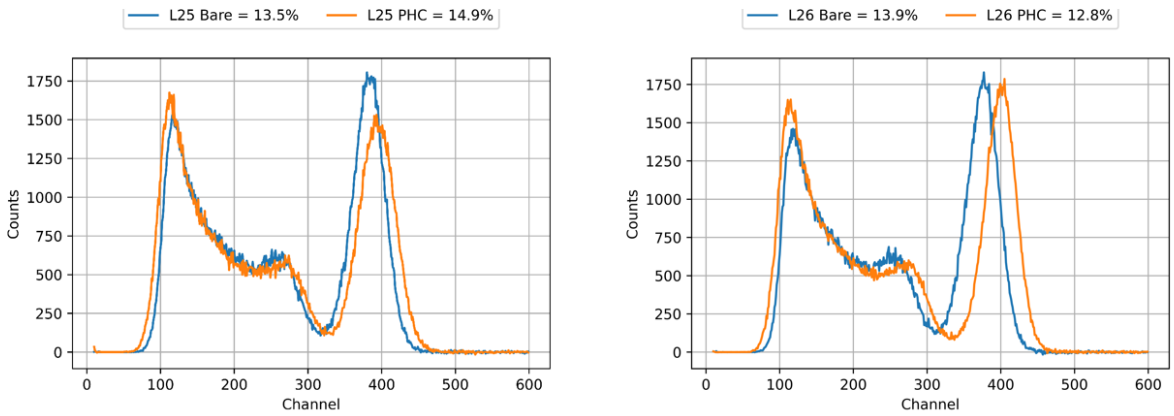

Figure 12. Radiation measurement for the LYSO PHC samples L25 (left) and L26 (right).

These preliminary results show that the light output increases in both crystals, although the effect is more prominent for L26 than for L25. For L25, the energy resolution slightly worsens with PHCs, from 13.5% for the bare scintillator to 14.9% for the PHC-coupled scintillator. For L26, the energy resolution improves, going from 13.9% for the bare scintillator to 12.8% for the PHC-coupled scintillator. While the two results are inconsistent, they indicate that even with a limited PHC coverage (60-70% of the LYSO surface) the PHC presence can improve the overall detection efficiency and energy resolution. Follow-up work is currently being done to achieve better and more consistent PHC coverage (90%+ with more consistent PHC dimensions) to assess the full potential of PHCs and their impact on the energy and time resolutions of various inorganic scintillators.

Conclusions

In previous work we have established a simulation procedure for optimizing the PHC structures of a wide range of scintillator materials and geometries. The simulated optimized Si_3N_4 PHC structures improve the light transmission in 10 x 10 x 3 mm^3 LYSO by ~63% for a single pass of light through the scintillator-photosensor interface. In this work, we manufactured first PHC geometries for LYSO using the electron beam lithography. Issues during the PHC manufacturing process were identified and will be corrected in future work. Specifically, samples L25 and L26 exhibited a varying PHC geometry with relatively poor PHC coverage. These flaws led to inconsistent results in the radiation measurements for the two samples. While the energy resolution worsened for L25, it was improved for L26. The results indicate that even with a limited PHC coverage (60-70% of the LYSO surface) the PHC presence can improve the overall detection efficiency and energy resolution.

The future work will target making the PHC manufacturing process repeatable with more than 90% PHC coverage. The electron beam process will also be optimized for the smaller PHC dimensions. In conjunction with this work, we are also exploring other PHC manufacturing techniques such as spin coating to produce polystyrene nanospheres. In the future, simulations and manufacturing efforts will also include other scintillator materials such as $LaBr_3$, which is estimated to have 73% TIR for a 25.4 x 25.4 x 3 mm^3 geometry.

Acknowledgements

This research is sponsored by the Defense Threat Reduction Agency (DTRA) of the Department of Defense (DOD) as part of the Interaction of Ionizing Radiation with Matter University Research Alliance (IIRM-URA) under contract number HDTRA1-20-2-0002.

References

[1] C. Dujardin *et al.*, "Needs, Trends, and Advances in Inorganic Scintillators," *IEEE Trans. Nucl. Sci.*, vol. 65, no. 8, pp. 1977–1997, 2018, doi: 10.1109/TNS.2018.2840160.

[2] M. Salomoni, R. Pots, E. Auffray, and P. Lecoq, "Enhancing Light Extraction of Inorganic Scintillators Using Photonic Crystals," *Crystals*, vol. 8, no. 2, Art. no. 2, Feb. 2018, doi: 10.3390/cryst8020078.

[3] P. Lecoq, E. Auffray, and A. Knapitsch, "How photonic crystals can improve the timing resolution of scintillators," in *2012 IEEE Nuclear Science Symposium and Medical Imaging Conference Record (NSS/MIC)*, Oct. 2012, pp. 4071–4075. doi: 10.1109/NSSMIC.2012.6551930.

[4] J. D. Joannopoulos, S. G. Johnson, J. N. Winn, and R. D. Meade, *Photonic crystals: Molding the flow of light*. Princeton University Press, 2011. Accessed: Dec. 08, 2023. [Online]. Available: https://collaborate.princeton.edu/en/publications/photonic-crystals-molding-the-flow-of-light

[5] S. Surani, F. Logoglu, P. Albert, D. Wolfe, and M. Flaska, "Inorganic scintillator surface enhancements with 2-D photonic crystals to improve light collection," *EPJ Web of Conferences*, vol. 288, p. 10014, Nov. 2023, doi: 10.1051/epjconf/202328810014.

[6] "LYSO Scintillation Crystals | Crystals." Accessed: Dec. 08, 2023. [Online]. Available: https://luxiumsolutions.com/radiation-detection-scintillators/crystal-scintillators/lyso-scintillation-crystals

[7] S. Agostinelli *et al.*, "Geant4—a simulation toolkit," *Nuclear Instruments and Methods in Physics Research Section A: Accelerators, Spectrometers, Detectors and Associated Equipment*, vol. 506, no. 3, pp. 250–303, Jul. 2003, doi: 10.1016/S0168-9002(03)01368-8.

[8] "OptiFDTD Overview," Optiwave. Accessed: Dec. 08, 2023. [Online]. Available: https://optiwave.com/optifdtd-overview/

[9] E. Dietz-Laursonn, "Peculiarities in the Simulation of Optical Physics with Geant4." arXiv, Dec. 15, 2016. Accessed: Dec. 08, 2023. [Online]. Available: http://arxiv.org/abs/1612.05162

[10] "OptiFDTD Technical Background and Tutorials." Optiwave, 2014. [Online]. Available: https://optiwave.com/download-1/optifdtd-10-technical-background-and-tutorials/

[11] "DT5730 / DT5730S," CAEN - Tools for Discovery. Accessed: Dec. 08, 2023. [Online]. Available: https://www.caen.it/products/dt5730/

[12] "CAEN Multi-PArameter Spectroscopy Software (CoMPASS)," CAEN - Tools for Discovery. Accessed: Dec. 08, 2023. [Online]. Available: https://www.caen.it/products/compass/